motion,[7] were observed. The vortex wake expanded for oscillation frequencies less than the Kármán frequency, whereas it contracted for frequencies greater than the Kármán frequency. The longitudinal spacing decreased significantly with increasing oscillation frequency and changed to a much lesser degree with an increase in the oscillation amplitude. In contrast, the lateral spacing of the shed vortices showed a relatively weaker dependence on the rotary oscillation. Further experiments on the vortex strength and formation are needed to better understand the characteristics of the various synchronized wake patterns.

References

[1]Tenada, S., "Visual Observations of the Flow past a Circular Cylinder Performing a Rotary Oscillation," *Journal of Physics Society of Japan*, Vol. 45, 1978, pp. 1038–1043.

[2]Filler, J. R., Marston, P. L., and Mih, W. C., "Response of the Shear Layers Separating from a Circular Cylinder to Small-Amplitude Rotational Oscillation," *Journal of Fluid Mechanics*, Vol. 231, 1991, pp. 481–499.

[3]Tokumaru, P. T., and Dimotakis, P. E., "Rotary Oscillation Control of a Cylinder Wake," *Journal of Fluid Mechanics*, Vol. 224, 1991, pp. 77–90.

[4]Fujisawa, N., Kawaji, Y., and Ikemoto, K., "Feedback Control of Vortex Shedding from a Circular Cylinder by Rotational Oscillations," *Journal of Fluids and Structures*, Vol. 15, 2001, pp. 23–37.

[5]Griffin, O. M., and Ramberg, S. E., "The Vortex-Street Wakes of Vibrating Cylinders," *Journal of Fluid Mechanics*, Vol. 66, 1974, pp. 553–576.

[6]Gerrard, J. H., "The Mechanisms of the Formation Region of Vortices Behind Bluff Bodies," *Journal of Fluid Mechanics*, Vol. 25, 1966, pp. 401–413.

[7]Williamson, C. H. K., and Roshko, A., "Vortex Formation in the Wake of an Oscillation Cylinder," *Journal of Fluids and Structures*, Vol. 2, 1988, pp. 355–381.

W. J. A. Dahm
Associate Editor

Pre-Limit-Point Buckling of Multilayer Cylindrical Panels Under Pressure

S. E. Rutgerson* and W. J. Bottega†
Rutgers University, Piscataway, New Jersey 08854-8058

I. Introduction

THIN shell structures, whether isotropic or composite, are seen in a wide variety of applications. In many situations the primary consideration is that of buckling of shell structures, particularly because of distributed (pressure) loads and point loads. An interesting, and perhaps common, phenomenon seen experimentally[1] is the onset of snap-through well below the limit load for force controlled tests. Pre-limit-point behavior is discussed analytically by Thompson and Hunt,[2] Simitses,[3] and by Pi and Trahair[4] for isotropic structures, but is often overlooked in many analyses. More recently, pre-limit-point buckling was identified for thermally loaded multilayer shell segments by Rutgerson and Bottega.[5]

In the present Note, buckling behavior of multilayer shallow shell segments subjected to external pressure is considered for plane-strain (long panel)/plain-stress (shallow arch) configurations with either clamped-fixed or pinned-fixed support conditions. The mathematical model, mixed formulation, and solution techniques presented and employed in Ref. 5 are applied to the present problem. It is shown that critical behavior, in the form of pre-limit-point snap-through buckling, is a function of a length ratio and a stiffness ratio of the composite structure. It is seen from numerical simulations that when snap-through buckling occurs it occurs below the limit load, often at values well below those that would be predicted from the limit point and that such behavior is pervasive.

II. Problem Statement

Consider the multilayer shell shown in Fig. 1. The structure will be considered to be composed of n layers, with the innermost layer of the composite shell denoted as layer 1 and the outermost layer as layer n. A convenient surface, say the interface between two layers or the geometric center of the structure, is used as the reference surface, and all length scales are normalized with respect to the dimensional radius of the undeformed reference surface. In doing so, the structure is described by the angular coordinate θ measured from the center of the span, and the half-length of the structure is defined by the angle ϕ^*. The structure is thus defined over the domain $-\phi^* \le \theta \le \phi^*$. A shallow shell theory is used as the mathematical model for each layer.[5]

The problem is stated in a mixed formulation in terms of the (normalized) radial displacement $w(\theta)$ (positive toward center of curvature) and the (normalized) resultant membrane force $\hat{N}$ (positive in compression). The equations and boundary conditions of Ref. 5 are applied to the present problem and are presented here. Hence,

$$w'''' + (2 + \hat{N})w'' + w = \hat{p} - (1 - \rho^*)\hat{N}, \qquad \theta \in [0, \phi^*] \tag{1a}$$

$$\hat{N}' = 0, \qquad \theta \in [0, \phi^*] \tag{1b}$$

$$w'(0) = 0 \tag{2a}$$

$$[w''' + (1 + \hat{N})w']_{\theta=0} = 0 \tag{2b}$$

$$w(\phi^*) = 0 \tag{2c}$$

$$w'(\phi^*) = 0 \tag{2d$_1$}$$

or

$$[w'' + w]_{\theta=\phi^*} = 0 \tag{2d$_2$}$$

where a superposed prime indicates total differentiation with respect to θ. Further, $\hat{p}$ is the nondimensional pressure and $\hat{N}$ is

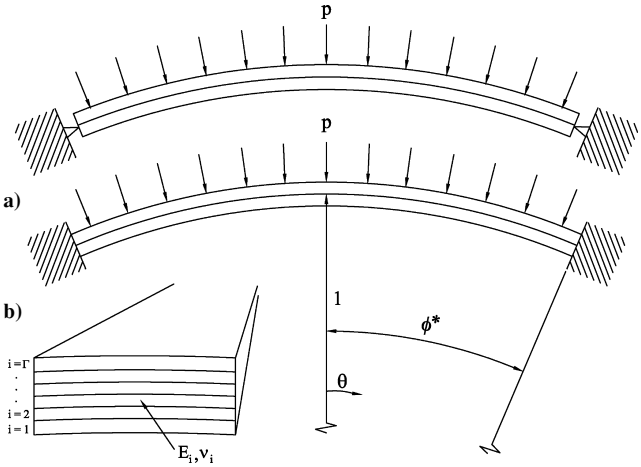

Fig. 1 Multilayer shell: a) pinned-fixed supports and b) clamped-fixed supports.

Received 17 January 2002; revision received 12 August 2003; accepted for publication 5 February 2004.

*Graduate Student; currently Structural Engineer, Naval Surface Warfare Center, Carderock Division, West Bethesda, MD 20817-5700.

†Associate Professor, Department of Mechanical and Aerospace Engineering. Associate Fellow AIAA.

the nondimensional membrane force. They are respectively defined in terms of their dimensional counterparts $\bar{p}$ and $\bar{N}^*$ by the relations

$$\hat{p} \equiv p/D^* = \left(\bar{p}\,\bar{R}^2/\bar{D}_1\right)/D^* \tag{3a}$$

$$\hat{N} \equiv -N^*/D^* = -\left(\bar{N}^*\,\bar{R}^2/\bar{D}_1\right)/D^* \tag{3b}$$

where D^* is a nondimensional composite stiffness,[5] $\rho^*(\ll 1)$ is a stiffness ratio,[5] $\bar{R}$ is the dimensional radius of the reference surface, and $\bar{D}_1$ is the dimensional bending stiffness of the innermost layer. The corresponding constitutive relations and definitions of stiffness parameters are omitted here for brevity but can be found in Ref. 5.

Integration of the constitutive relation for the membrane force[5] over $[0, \phi^*]$ and applying the boundary conditions associated with the circumferential deflection at the centroidal surface[5] gives the integrability condition

$$\frac{-\hat{N}\phi^*}{C^*/D^*} + (1-\rho^*)\int_0^{\phi^*} w\,\mathrm{d}\theta - \frac{1}{2}\int_0^{\phi^*} w'^2\,\mathrm{d}\theta = 0 \tag{4}$$

where the parameters C^* and D^* correspond to stiffnesses of the composite structure as defined in Ref. 5. Equations (1–4) define the mixed formulation in terms of the transverse deflection $w(\theta)$ and the uniform resultant membrane force $\hat{N}$. As $\rho^* \ll 1$, it can be seen that the material parameters effectively enter the problem through the ratio C^*/D^* in the integrability condition. The formulation and normalization employed is therefore seen to provide a universal statement of the problem in that the equations, and hence the corresponding results are effectively the same for monolayer structures, bilayer structures, and multilayer structures having the same stiffness ratio.

III. Analysis

Equations (1a) and (b) together with boundary conditions (2a–2d) are solved analytically giving the solution for the radial displacement in the form[5]

$$w(\theta) = \hat{Q}W(\theta;\hat{N}) = \hat{Q}[G(\theta;\hat{N})/F_0(\phi^*;\hat{N}) + 1] \tag{5}$$

where

$$\hat{Q} = \hat{p} - (1-\rho^*)\hat{N} \approx \hat{p} - \hat{N} \tag{6}$$

The specific forms of the functions G and F_0 depend on the boundary conditions and can be found in Ref. 5, for both clamped-fixed and pinned-fixed support conditions.

Stability of an equilibrium configuration is assessed by examination of the second variation of the total potential energy of the system for arbitrary perturbations. It is shown in Ref. 5 that assessing stability of an equilibrium configuration reduces to consideration of the positive definiteness of the stability function F^*, defined by the relation

$$F^* = F^*(N_0) \equiv \int_0^{\phi^*} \frac{D^*}{2\hat{N}_0}[W''(\theta;\hat{N}_0) + W(\theta;\hat{N}_0)]^2\,\mathrm{d}\theta - \frac{1}{2}\int_0^{\phi^*} W'^2(\theta;\hat{N}_0)\,\mathrm{d}\theta \tag{7}$$

where $\hat{N}_0$ represents the particular value of the membrane force $\hat{N}$ at the equilibrium configuration in question. The stability criterion thus takes the following form:

$$\text{An equilibrium configuration is stable if } F^* > 0 \tag{8}$$

It is unstable otherwise.

Substitution of the solution (5), for the particular boundary conditions of interest, into Eq. (4) and carrying through the indicated operations results in a transcendental equation for the membrane force $\hat{N}$ as a function of the applied pressure $\hat{p}$ for given values of the stiffness ratio C^*/D^* and the half-length ϕ^*. This equation can then be solved numerically, using root solving techniques,

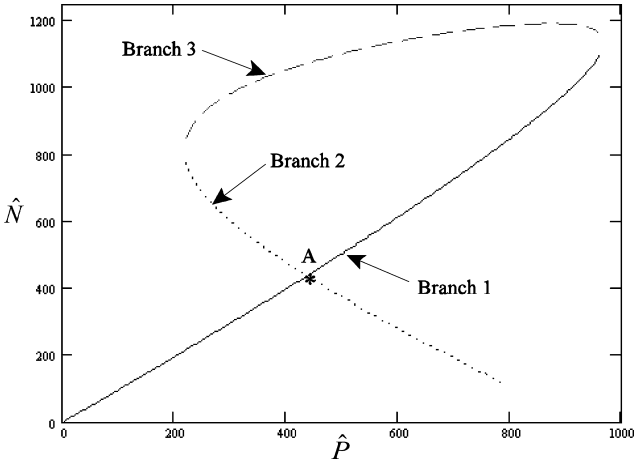

a)

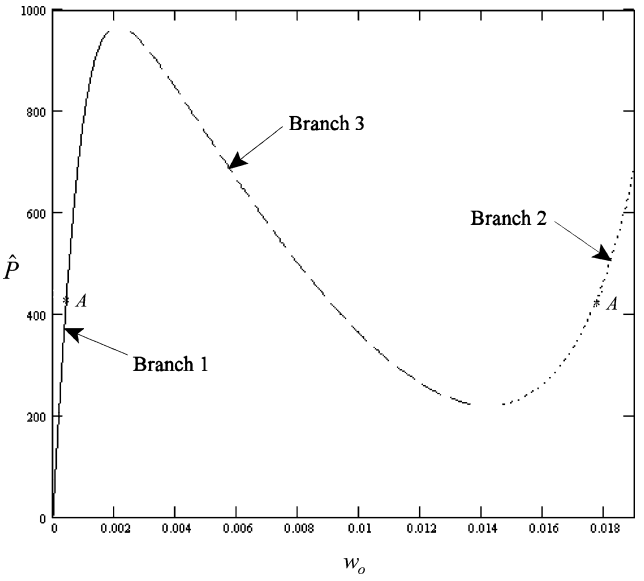

b)

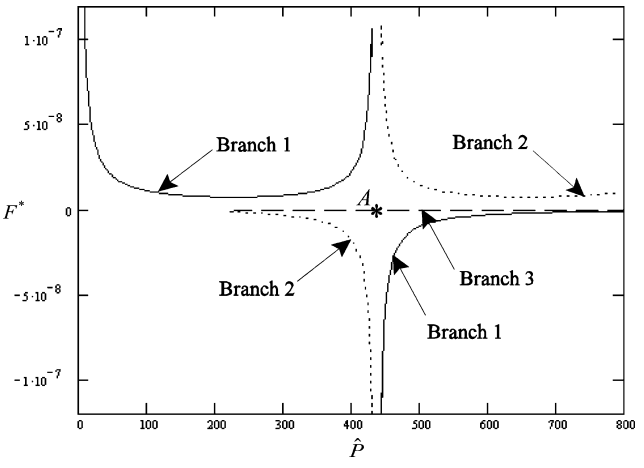

c)

Fig. 2 Behavior of structure with clamped-fixed supports ($\phi^* = 0.15$, $C^*/D^* = 2 \times 10^6$): a) roots of integrability condition, b) applied pressure vs transverse centerspan deflection, and c) stability function vs applied pressure.

yielding values of the membrane force associated with equilibrium configurations of the deforming structure. When multiple roots are found for a given value of the applied pressure, stability of the corresponding equilibrium configurations will be assessed using the criterion (8).

From the corresponding discussion of Ref. 5, the critical membrane force and critical pressure are found as the roots of vanishing F_0 and simultaneous vanishing of F_0 and $\hat{Q}$, respectively. Hence,

$$F_0(\hat{N};\phi^*) = 0 \Rightarrow \hat{N}_{\text{cr}} \tag{9}$$

where $\hat{N}_{\text{cr}}$ corresponds to the lowest roots of Eq. (8) and is designated as the critical membrane force, and

$$F_0 = 0, \qquad \hat{Q} = 0 \Rightarrow \hat{p}_{\text{cr}} = (1-\rho^*)\hat{N}_{\text{cr}} \approx \hat{N}_{\text{cr}} \tag{10}$$

where $\hat{p}_{\text{cr}}$ is designated as the critical pressure. With the exception of the half-length of the span, the critical normalized membrane force is seen to be independent of the material and geometric properties of the structure. This is seen to (effectively) be the case for the critical pressure as well.

IV. Results

Representative results of numerical simulations, based on the analytical solutions discussed in Sec. III, are presented for clamped-fixed support conditions. Results for pinned-fixed support conditions show similar critical behavior and are omitted for brevity. Roots of the explicit form of the integrability condition (4) are found numerically via a hybrid method composed of an incremental step-based root finding algorithm and the bisection technique. Stability is then assessed using the criterion established earlier. In what follows, the transverse centerspan deflection is identified as the characteristic deflection and is denoted as w_0. Thus, $w_0 \equiv w(0)$.

Sample results are presented in Figs. 2a and 2b for a representative structure of half-length $\phi^* = 0.15$ and stiffness ratio $C^*/D^* = 2 \times 10^6$. The roots of the integrability condition (4) for this case are displayed as a function of the applied pressure in Fig. 2a, where the first three branches associated with the first three roots are identified and numbered sequentially. It can be observed that the first two branches cross at the point labeled A and that this occurs when $\hat{N} = \hat{N}_{\text{cr}}$ and $\hat{p} = \hat{p}_{\text{cr}}$ as defined at the end of the preceding section. The crossing implies that, at this point, two equilibrium configurations are associated with this value of the membrane force (root of the integrability condition). The two equilibrium configurations associated with points A of the branch crossing are also indicated on the corresponding load-deflection path displayed in Fig. 2b. On the basis of the stability criterion defined by Eq. (8), it is found that the equilibrium configurations associated with the first branch are stable upon initial loading but become unstable after the applied pressure reaches the critical value associated with point A. It is also found that the equilibrium configurations associated with the second branch become stable beyond this pressure level, having been unstable for pressures below the critical value (see Fig. 2c). Thus, the results imply that when $\hat{p} = \hat{p}_{\text{cr}}$ the structure undergoes snap-through buckling to the corresponding deflection indicated by point A on branch 2 of the load-deflection path (Fig. 2b). It is seen that such buckling occurs well below the limit load for this case. (Such behavior was observed in the experiments of Marshall et al.[1] for an isotropic shell under slightly different conditions.)

The existence of prelimit point snap-through buckling is seen to be a function of the geometrical and material properties of the structure. In particular, pre-limit-point snap-through is a function of the stiffness ratio C^*/D^* and the span half-length ϕ^*. Plots of the roots of the integrability condition for two structures of the same length ($\phi^* = 0.10$), but with differing stiffness ratios ($C^*/D^* = 2 \times 10^6$ and $C^*/D^* = 5 \times 10^5$), are compared in Fig. 3. The first plot shows root crossing, indicating pre-limit-point buckling, whereas the second plot does not. A continuous variation of the stiffness ratio (not presented) shows a continuous variation of trend between these two states, characterized by a monotonic decrease of area of the loop compared with the area under the crossing. Correspondingly, when the branch crossing (point A) disappears so does the peak in the load-deflection curve. In this event, it is observed that the associated portion of the equilibrium path becomes effectively flat implying incremental static buckling. Thus, in the strict sense for the class of laminated shallow shell structures considered the presence of a peak or limit load implies the possibility of snap-through buckling. However, for the cases considered snap-though was observed to always occur before the limit load was achieved. Similar trends are found when the span length is varied while fixing the stiffness ratio ($C^*/D^* = 2 \times 10^6$). In this regard, a comparison of load-deflection curves the critical point A is shown for various span lengths in Fig. 4.

V. Summary

The response of single- and multilayer shallow shells in plane stress/plane strain configurations has been studied for structures subjected to radial pressure applied to the outer surface of the shell. A stability criterion based on the second variation of the total potential energy was established, critical parameters identified, and closed-form analytical solutions to the nonlinear problem obtained.

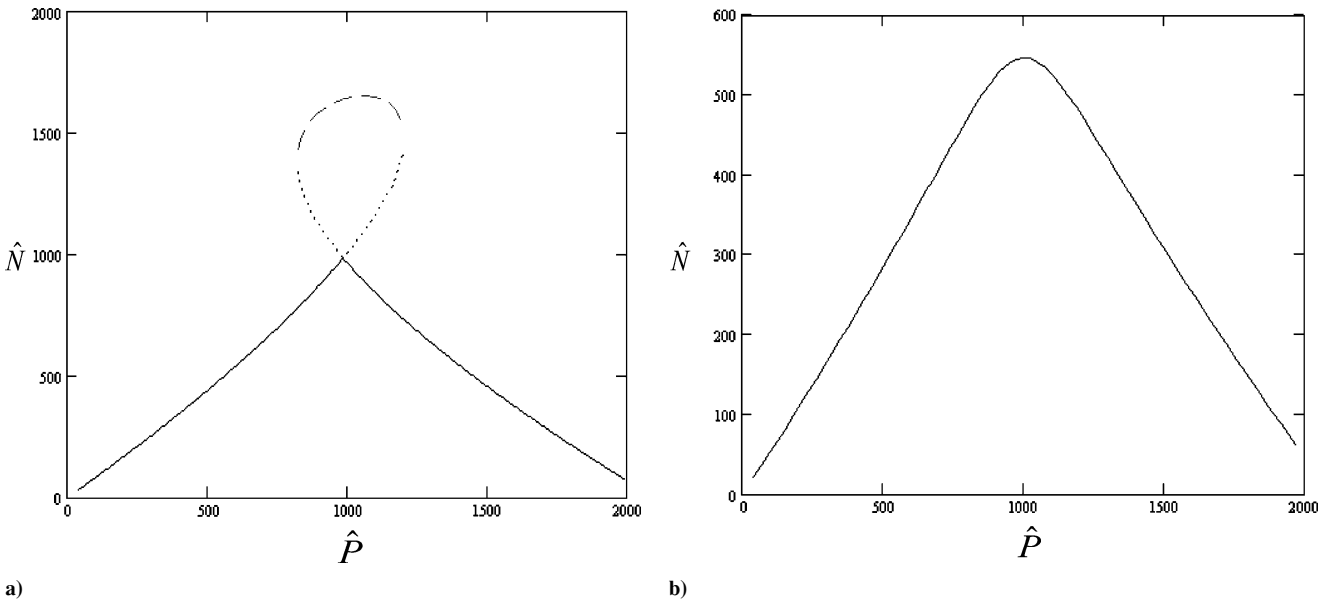

Fig. 3 Dependence of branch crossing on stiffness ratio (clamped-fixed supports, $\phi^* = 0.10$): a) $C^*/D^* = 2 \times 10^6$ and b) $C^*/D^* = 5 \times 10^5$.

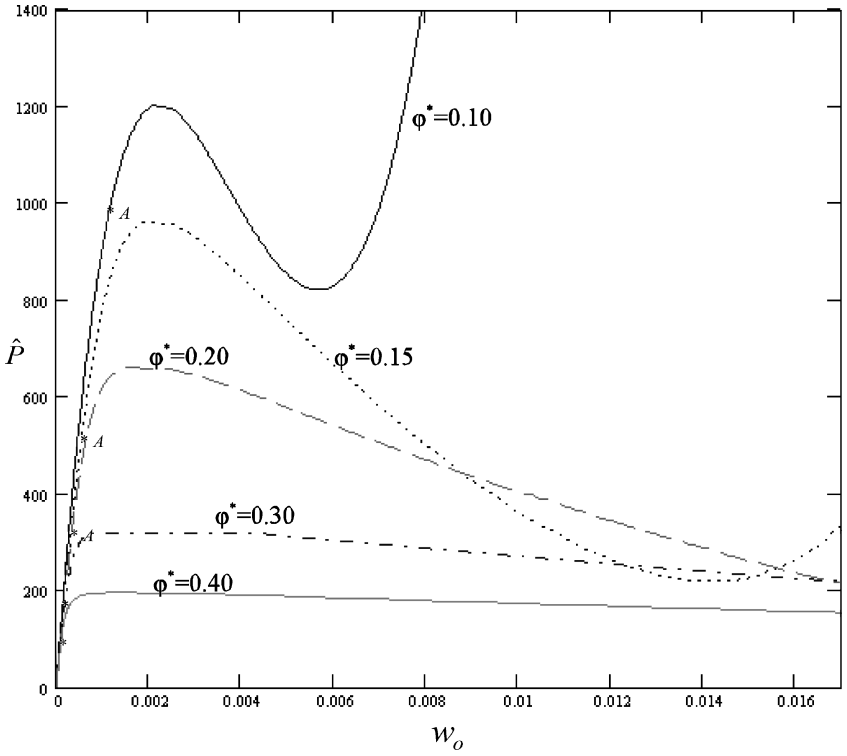

Fig. 4 Load-deflection paths for various (half) span lengths, showing dependence of critical pressure (clamped-fixed supports, $C^*/D^* = 2 \times 10^6$).

Numerical simulations, based on these analytical solutions, were performed and a stability analysis based on the aforementioned criterion was applied for various representative structures. Crossing of the first two branches corresponding to the roots (membrane forces) of the integrability condition was seen to be associated with critical behavior of the structure. In all cases it was seen that snap-through buckling occurred if the load-deflection path for the given point possessed a limit point. However, in all cases, such snap-through behavior was seen to occur below and typically well below the limit load. This pre-limit-point snap-through buckling was seen to be pervasive for the class of structures considered, whether single- or multilayer, having significant implications concerning conventional (limit-point) criteria with regard to buckling of shell structures under force controlled loading.

References

[1]Marshall, I. H., Rhodes, J., and Banks, W. M., "The Nonlinear Behavior of Thin, Orthotropic, Curved Panels Under Lateral Loading," *Journal of Mechanical Engineering Science*, Vol. 19, No. 1, 1977, pp. 20–37.

[2]Thompson, J. M. T., and Hunt, G. W., *A General Theory of Elastic Stability*, Wiley-Interscience, London, 1973, pp. 57–59.

[3]Simitses, G. J., *Elastic Stability of Structures*, Krieger, Malabar, FL, 1986, p. 190.

[4]Pi, Y.-L., and Trahair, N. S., "Non-Linear Buckling and Postbuckling of Elastic Arches," *Engineering Structures*, Vol. 20, 1998, pp. 571–579.

[5]Rutgerson, S. E., and Bottega, W. J., "Thermo-Elastic Buckling of Layered Shell Segments," *International Journal of Solids and Structures*, Vol. 39, 2002, pp. 4867–4887.

A. M. Waas
Associate Editor